

A general circulation model simulation of the Martian polar warming

R. John Wilson

Geophysical Fluid Dynamics Laboratory/NOAA, Princeton University, Princeton, New Jersey

Abstract. This paper reports on a successful general circulation model simulation of a rapid warming phenomenon observed in the Martian winter polar atmosphere during global dust storm conditions. The model includes a self-consistent simulation of the dust distribution which is forced with a prescribed surface source. The warming is shown to be largely a response to the development of a pole-to-pole solstitial Hadley circulation resulting from the greatly increased dust loading. A crucial aspect of the simulation is a sufficiently deep computational domain that allows for the full development of this circulation. These simulations indicate that the thermal tides play a contributing role by providing zonal momentum flux divergence at the winter pole and by the advection of aerosol.

Introduction

An interesting aspect of Martian atmospheric dynamics is the large variability in amount and distribution of radiatively active aerosol. This is most impressively evident during global dust storms when the dust haze can extend to heights of 60 km (Anderson and Leovy, 1978) over a large fraction of the planet, achieving column-integrated optical depths of 5-6 (Zurek, 1982). A particularly striking warming of the winter polar atmosphere was observed by the Infrared Thermal Mapper instrument (IRTM) aboard the Viking orbiters coincident with the onset of the 1977b global dust storm at northern hemisphere winter solstice (Martin and Kieffer, 1979; Jakosky and Martin, 1987). The observed $15\mu\text{m}$ brightness temperatures (T_{15}) represent a weighted average of the atmospheric temperature over a thick layer centered near 25 km (0.5 mb) altitude. Zonally-averaged pre-storm and storm temperatures are shown in Fig. 1. While the temperature increases in the summer (southern) hemisphere may be attributed to greater absorption of solar radiation due to dust, increases in the winter pole night must be a result of dynamical processes leading to strong subsidence in the zonal mean meridional circulation.

Haberle et al. (1982) employed a 2-D model with aerosol transport to explore the possibility that the warming may be due to a meridional expansion of the Hadley circulation in response to increased aerosol heating. These calculations demonstrated that this circulation intensifies with increasing dust loading and is capable of lofting dust high in the summer hemisphere and rapidly transporting it into the winter hemisphere under dust storm conditions. Subsequent simulations with the NASA/Ames Mars GCM (Haberle et al. 1993; Mur-

phy et al., 1995) have corroborated these results and shown that the Hadley circulation is a prominent component of the Martian general circulation, particularly during the solstice seasons. However the winter polar temperatures remained near radiative equilibrium (~ 140 K) in all cases. The simulations were carried out with the model top at a relatively shallow height of ~ 50 km which evidently was shallow enough to require dissipation (Rayleigh drag) for model stability. The polar warming phenomenon is re-examined here using a newly developed Martian GCM (Wilson and Hamilton, 1996; hereafter WH96) that features aerosol transport and a deeper model domain.

Solstitial Hadley Circulation

Mars GCM results are consistent with theoretical expectations for the behavior of a nearly-inviscid Hadley circulation based on the conservation of absolute angular momentum (e.g. Held and Hou, 1980). A notable aspect of agreement is that the circulation intensity is strongly sensitive to the seasonally varying latitude of maximum radiative forcing (Lindzen and Hou, 1988; Dunkerton, 1989). For the case in which the radiative equilibrium temperature decreases monotonically from the summer pole to the winter pole, Schneider (1983) demonstrated the possibility of a "solstitial Hadley circulation"; a thermally-direct meridional cell extending from the summer pole to the winter pole. Such a circulation yields strong depth-averaged easterlies in the tropics and westerlies in the winter hemisphere as is consistent with angular momentum conservation.

Schneider suggested that an important consideration for modelling this circulation is the potential for inertial instability if the numerical domain is insufficiently deep for a given horizontal (pole-to-pole) temperature contrast. This is a consequence of the large vertical shear in the zonal wind created by the upper branch of the meridional circulation. In such a case numerical stability requires introducing dissipation which relaxes the constraint of conservation of angular momentum and fundamentally alters the character of the circulation so that it is controlled by the diffusion rather than by inertial effects.

The model employed for this study is based on the GFDL SKYHI terrestrial GCM (Hamilton et al. 1995) and is essentially that described in WH96. The model now incorporates the CO_2 condensation circulation, and the optical properties of the aerosol are those suggested by Clancy et al. (1995). Two versions of the GCM were discussed in WH96, one with 16 numerical levels up to ~ 70 km and one with 40 levels up to ~ 90 km. WH96 noted that increasing the domain height, which enabled a decreasing of the Rayleigh drag, led to increasingly warmer winter polar temperatures. Subsequent integrations of the model have shown that by placing the top

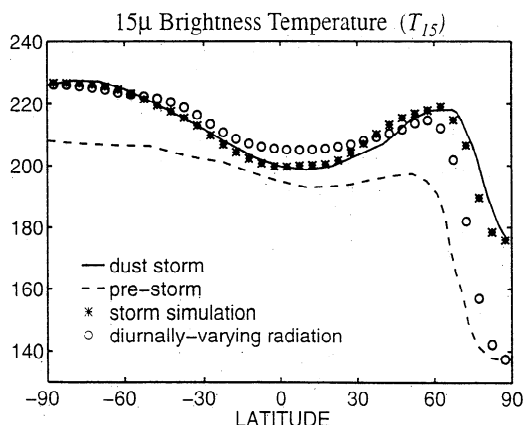


Figure 1. Latitudinal profiles of T_{15} for the periods preceding ($L_s=250-270^\circ$) and following ($L_s=274-290^\circ$) the onset of the 1977b global dust storm. Time of year is represented by the areocentric longitude, L_s , which is defined to be zero at the vernal equinox, 90° at northern hemisphere summer solstice etc. Simulated profiles of T_{15} are also shown. These were synthesized by converting model temperatures to radiances, sampling these by the IRTM instrument vertical weighting function and converting back to temperature.

above ~ 80 km, the model may be stably integrated without arbitrary dissipation for any reasonable radiative forcing. This behavior is also evident in an axisymmetric version of the GCM and is independent of the choice of model time step.

Dust Storm Simulation Results

Simulations with the present model employing fixed, horizontally uniform aerosol distributions yield roughly realistic winter pole T_{15} temperatures for column-integrated optical depths of unity and even higher temperatures for more realistic dust storm optical depths. It is not obvious, however, that such an idealized aerosol distribution is very realistic and it is likely that the Hadley response will show sensitivity to the depth and meridional extent of the dust. For this reason, the integrations described here employ dust transport which allows for a self-consistent simulation of the aerosol distribution given specified source and sink terms.

A globally-uniform injection of dust into the lowest model level is prescribed as a simple representation of surface dust raising during the development of a Martian dust storm. As discussed in WH96, the lofting of this dust into the free atmosphere is largely effected by the Hadley circulation and modulated by the large scale topography. For transport purposes, the aerosol is assumed to have a sedimentation velocity appropriate for a monodisperse distribution of spherical particles.

A number of scenarios have been considered for the temporal behavior of the dust source, ranging from a relatively weak but steady dust source initiated at autumnal equinox ($L_s=180^\circ$) to stronger, episodic events initiated near northern winter solstice ($L_s=270^\circ$). For equivalent dust loadings these simulations lead to comparable polar warmings, although with differing rates of onset and subsequent decay, suggesting that the warming phenomenon is not dependent on transient effects. The standard dust storm experiment presented here employs a strong episodic dust source peaking 8 sols after

initiation at $L_s=268^\circ$. This simulation used a sedimentation velocity corresponding to a particle radius of $0.9 \mu\text{m}$.

Latitude-height cross-sections of the simulated zonally-averaged temperature, zonal wind and aerosol mixing ratio fields are shown in Fig. 2 for dust storm conditions. The warm temperatures in both the summer and winter extratropics relative to those of the tropics is a characteristic response of a nearly-inviscid meridional circulation as discussed by Schneider (1983). The close agreement between the observed and simulated T_{15} temperatures is shown in Fig. 1.

The broad and deep distribution of aerosol mixing ratio (Fig. 2c) is consistent with observations of the dust haze height near the peak of the 1971 global dust storm as deduced by Anderson and Leovy (1978). The column-integrated optical depth is ~ 6 , comparable to the best estimates for the 1977b global dust storm (Zurek, 1982). The latitude vs. local time variation of simulated T_{15} is in good agreement with the IRTM observations (Martin and Kieffer, 1979), suggesting that the strength of the aerosol-induced heating is well simulated.

The zonal mean zonal winds (Fig. 2b) undergo significant change as the simulated dust storm evolves. Most prominently, the tropical upper level easterlies intensify greatly in response to the development of an angular momentum conserving summer-pole-to-winter-pole meridional circulation. At high altitudes the zonal wind distribution has the parabolic form consistent with such a circulation, with equatorial

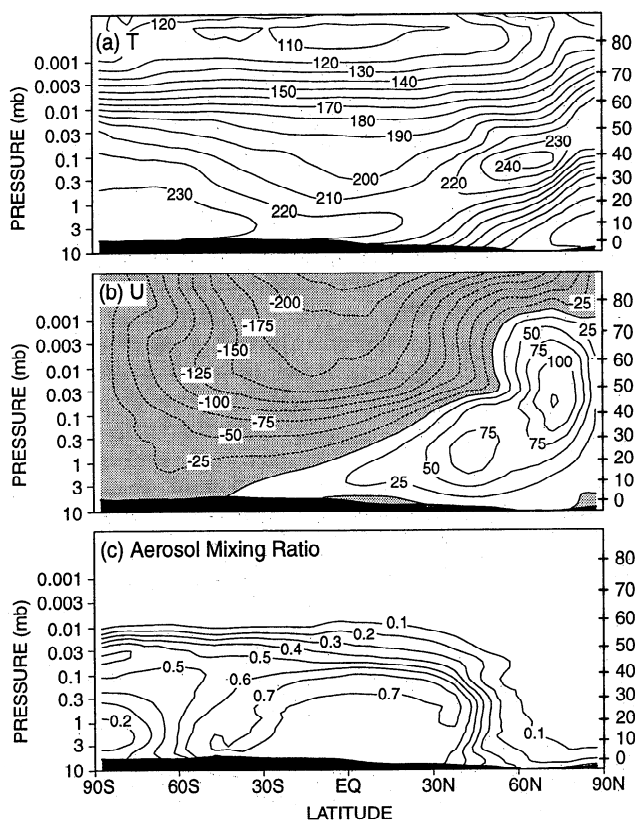


Figure 2. Latitude-height sections of zonally averaged (a) temperature, (b) zonal wind and (c) aerosol mass mixing ratio averaged over 5 sols (a Martian solar day, equal to 88775 sec.) at the peak of the simulated dust storm. Temperature in degrees Kelvin. Zonal wind velocity in ms^{-1} .

winds achieving velocities approaching the limiting value of $a\Omega = -240 \text{ ms}^{-1}$ where a and Ω are the planetary radius and rotational frequency.

The simulated near-surface winds corresponding to the Viking Lander 2 site at 48°N undergo a shift from westerly to northeasterly as the dust loading is increased, in agreement with observations (Ryan and Henry, 1979) following the 1977b dust storm. Notably this shift is absent in simulations without a significant polar warming.

A dust storm simulation was also carried out with a version of the model employing diurnally-averaged radiation so as to exclude the thermal tides. In this simulation the winter pole T_{15} temperature remained near radiative equilibrium as seen in Fig. 1. Although the dust loading throughout the tropics and subtropics is very similar in the two simulations, the spreading of aerosol over the southern polar latitudes seen in Fig. 2c is absent in the simulation without thermal tides.

Interpretation and Discussion

The two panels of Fig. 3 contrast aspects of the zonal mean circulation for the standard simulation with those for the simulation employing diurnally-averaged radiation. Each panel shows contours of zonally-averaged meridional mass transport stream function and absolute angular momentum (M -surfaces). The shading indicates regions of significant

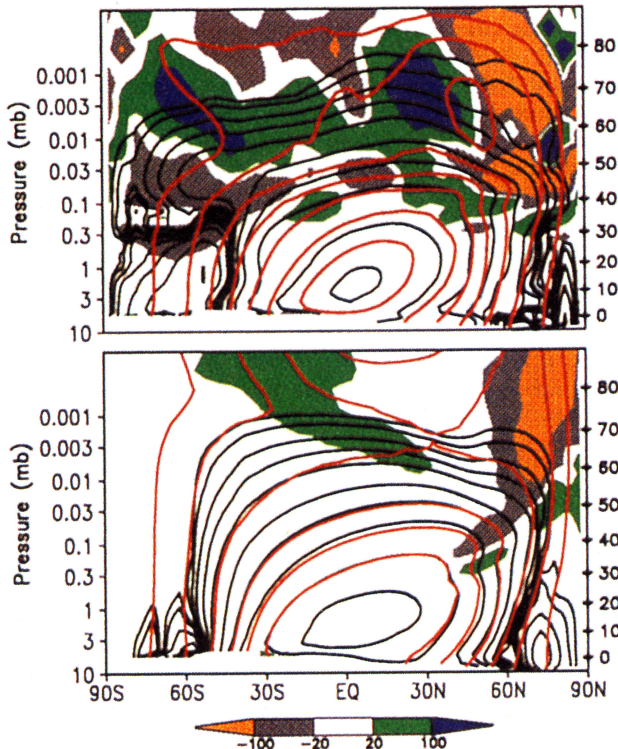


Figure 3. Time-mean zonal-mean meridional streamfunction (black contours) and absolute angular momentum (red contours) for (a) the standard dust storm simulation and (b) a simulation with diurnally-averaged radiation. Streamfunction contour intervals are logarithmic with positive values indicating clockwise circulation. Shaded regions indicate momentum flux divergence with positive values corresponding to zonal momentum acceleration. Units are in $\text{ms}^{-1}\text{sol}^{-1}$.

momentum forcing by acceleration terms (dissipation and eddy momentum flux divergence) in the zonal momentum balance equation. In the absence of these terms, the meridional circulation must be parallel to the M -surfaces as a consequence of conservation of angular momentum.

To the extent that the stream function and M -surfaces are roughly parallel over a large region of the atmosphere, the thermally-direct cell implied by the stream function is consistent with the inertially-controlled "solstitial circulation" proposed by Schneider (1983). This may be contrasted with the terrestrial middle atmosphere where the meridional circulation is largely induced by dissipation associated with planetary and gravity waves (Andrews et al. 1987).

The meridional circulation in the standard dust storm simulation (Fig. 3a) is further broadened by these acceleration terms so that a pole-to-pole circulation is achieved. A detailed examination of the zonal momentum balance reveals that the shaded regions in Fig. 3a are strongly dominated by momentum flux divergence associated with the thermal tides. The zonal wavenumber 1 component of the diurnal tide has a peak amplitude near 80°N . The fact that the thermal tides have such an effect at winter polar latitudes is not expected in the context of classical tidal theory, (Zurek, 1986; Zurek and Haberle, 1988) but is a result of the strong zonal winds as has been noted in WH96. Note that the momentum flux divergence due to the tides accounts for the advection of aerosol over the south pole noted previously. This southward transport is absent in the simulation without tides, consistent with the stream function shown in Fig. 3b.

A notable aspect of the simulated circulation is the virtually uniform, near-zero distribution of potential vorticity throughout much of the atmosphere, with an area of strong meridional gradient tightly confined about the winter pole. The acceleration terms shown in Fig. 3b are likely a result of inertial instability, however further analysis is needed to confirm this.

In the diurnal mean, the polar vortex retains a high degree of axisymmetry throughout the warming. In fact, the simulations show a marked reduction in transient (non-tidal) and stationary wave activity as the polar warming develops. The relative insignificance of planetary scale waves for the simulated polar warming is in contrast to the case of the terrestrial stratospheric sudden warming (e.g. Andrews et al., 1987) where the transience of forced, near-stationary planetary waves leads to a highly disturbed polar vortex. The possible analogy with the terrestrial case had been presented by Barnes and Hollingsworth (1987).

An intriguing aspect of the 1977b dust storm IRTM data is a large amplitude day/night temperature variability that peaks at $\sim 80^\circ\text{N}$ (Jakosky and Martin, 1987). While interpretation of the data is made difficult by sampling limitations (at best, only two longitudes per day were viewed as a result of the asynchronous orbits), the simulation results suggest that the thermal tides, coupled with small off-pole displacements of the polar vortex, yields temperature variability not inconsistent with the observations.

Conclusion

These simulations indicate that the polar warming phenomenon is a result of the development of the solstitial Hadley circulation, the strength of which increases as the thermal forcing becomes increasingly asymmetric about the equator.

This asymmetry is due to both the seasonally varying solar geometry and the evolving aerosol distribution. In simulations with fixed, uniformly mixed aerosol, polar warmings were localized about the time of solstice, consistent with a weakening of the Hadley circulation away from solstice. Consistent with the sedimentation of the micron-sized particles and the assumed time variation of the dust source, the simulated polar warming decayed rapidly after $L_s=300^\circ$ in agreement with the IRTM observations (Jakosky and Martin, 1987). The height of the simulated dust haze decreased most rapidly over the south pole during the decaying stages of the dust storm consistent with the observations of Anderson and Leovy (1978). No polar warming is evident in the IRTM data at the time of the earlier 1977a global dust storm ($L_s\sim 205^\circ$, well before solstice) although temperatures did rise significantly at more southerly extratropical latitudes.

The thermal tides contribute to the polar warming by providing sufficient momentum flux divergence to enable the meridional circulation to extend beyond 70°N to the winter pole. They also contribute by inducing increased radiational heating at far southerly latitudes (by aerosol transport) and dynamical heating near the summer pole, thereby strengthening the solstitial Hadley circulation. The thermal tides represent a significant source of feedback as their strength and ability to advect aerosol varies with the optical depth of the atmosphere.

Acknowledgments. The author would like to thank Mark Richardson for providing a routine for computing T_{15} temperatures. Further thanks are extended to Francois Forget and Terry Martin for supplying IRTM data. The author is also grateful to Kevin Hamilton, Paul Kushner, Isaac Held, Jerry Mahlman, and the reviewers for comments on the manuscript.

References

- Anderson, E., and C. Leovy, Mariner 9 television limb observations of dust and ice hazes on Mars, *J. Atmos. Sci.*, **35**, 723-734, 1978.
- Andrews, D.G., J.R. Holton, and C.B. Leovy, *Middle Atmosphere Dynamics*, 489 pp., Academic Press, 1987.
- Barnes, J.R., and J.L. Hollingsworth, Dynamical modeling of a planetary wave mechanism for a Martian polar warming, *Icarus*, **71**, 313-334, 1987.
- Clancy, R.T., S.W. Lee, G.R. Gladstone, W.W. McMillan, and T. Rousch, A new model for Mars atmospheric dust based upon analysis of ultraviolet through infrared observations from Mariner 9, Viking and Phobos, *J. Geophys. Res.*, **100**, 5251-5263, 1995.
- Dunkerton, T.J., Nonlinear Hadley Circulation Driven by Asymmetric Differential Heating, *J. Atmos. Sci.*, **46**, 956-974, 1989.
- Haberle, R.M., C.B. Leovy and J.B. Pollack, Some effects of global dust storms on the atmospheric circulation of Mars, *Icarus*, **50**, 322-367, 1982.
- Haberle, R.M., J.B. Pollack, J.R. Barnes, R.W. Zurek, C.B. Leovy, J.R. Murphy, H. Lee, and J. Schaeffer, Mars atmospheric dynamics as simulated by the NASA Ames General Circulation Model 1. The zonal mean circulation, *J. Geophys. Res.*, **98**, 3093-3123 1993.
- Hamilton, K., R.J. Wilson, J.D. Mahlman, and L.J. Umscheid, Climatology of the SKYHI troposphere-stratosphere-mesosphere general circulation model, *J. Atmos. Sci.*, **52**, 5-43, 1995.
- Held, I.M., and A.Y. Hou, Nonlinear axially symmetric circulations in a nearly inviscid atmosphere, *J. Atmos. Sci.*, **26**, 841-853., 1980.
- Jakosky, B.M., and T.Z. Martin, Mars: North-polar atmospheric temperatures during dust storms, *Icarus*, **72**, 528-534, 1987.
- Lindzen, R.S., and A.Y. Hou, Hadley circulations for zonally-averaged heating centered off the equator, *J. Atmos. Sci.*, **45**, 2416-2427, 1988.
- Martin, T.Z., and H. Kieffer, Thermal infrared properties of the Martian atmosphere. 2. The $15\ \mu\text{m}$ band measurements, *J. Geophys. Res.*, **84**, 2843-2852, 1979.
- Murphy, J.R., R.M. Haberle, O.B. Toon, and J.B. Pollack, Martian global dust storms: Zonally symmetric numerical simulations including size-dependent particle transport, *J. Geophys. Res.*, **98**, 3197-3220, 1993.
- Murphy, J.R., J.B. Pollack, R.M. Haberle, C.B. Leovy, O.B. Toon, and J. Schaeffer, Three dimensional numerical simulation of Martian global dust storms, *J. Geophys. Res.*, **100**, 26357-26376, 1995.
- Ryan, J.A., and R.M. Henry, Mars atmospheric phenomena during major dust storms, as measured at the surface, *J. Geophys. Res.*, **84**, 2821-2829, 1979.
- Schneider, E.K., 1983: Martian great dust storms: Interpretive axially symmetric models, *Icarus*, **55**, 302-331.
- Wilson, R.J., and K. Hamilton, Comprehensive model simulation of thermal tides in the Martian atmosphere, *J. Atmos. Sci.*, **53**, 1290-1326, 1996.
- Zurek, R.W., Martian great dust storms: An update, *Icarus*, **50**, 288-310, 1982.
- Zurek, R.W., Atmospheric tidal forcing of the zonal-mean circulation: The Martian dusty atmosphere, *J. Atmos. Sci.*, **43**, 652-670, 1986.
- Zurek, R.W., and R.M. Haberle, Zonally symmetric response to atmospheric tidal forcing in the dusty Martian atmosphere, *J. Atmos. Sci.*, **45**, 2469-2485, 1988.

R. J. Wilson, NOAA/GFDL, PO Box 308, Princeton, NJ 08542 (e-mail: rjw@gfdl.gov)

(Received October 10, 1996; revised December 4, 1996; accepted December 11, 1996.)